Todyformer: Towards Holistic Dynamic Graph Transformers with Structure-Aware Tokenization

Mahdi Biparva[*]
Huawei Noah's Ark Lab
Toronto, Canada

Raika Karimi [*]
Huawei Noah's Ark Lab
Toronto, Canada

Faezeh Faez
Huawei Noah's Ark Lab
Toronto, Canada

Yingxue Zhang
Huawei Noah's Ark Lab
Toronto, Canada

Abstract

Temporal Graph Neural Networks have garnered substantial attention for their capacity to model evolving structural and temporal patterns while exhibiting impressive performance. However, it is known that these architectures are encumbered by issues that constrain their performance, such as over-squashing and over-smoothing. Meanwhile, Transformers have demonstrated exceptional computational capacity to effectively address challenges related to long-range dependencies. Consequently, we introduce Todyformer—a novel Transformer-based neural network tailored for dynamic graphs. It unifies the local encoding capacity of Message-Passing Neural Networks (MPNNs) with the global encoding of Transformers through i) a novel patchifying paradigm for dynamic graphs to improve over-squashing, ii) a structure-aware parametric tokenization strategy leveraging MPNNs, iii) a Transformer with temporal positional-encoding to capture long-range dependencies, and iv) an encoding architecture that alternates between local and global contextualization, mitigating over-smoothing in MPNNs. Experimental evaluations on public benchmark datasets demonstrate that Todyformer consistently outperforms the state-of-the-art methods for downstream tasks. Furthermore, we illustrate the underlying aspects of the proposed model in effectively capturing extensive temporal dependencies in dynamic graphs.

1 Introduction

Dynamic graphs, driven by the surge of large-scale structured data on the internet, have become pivotal in graph representation learning. Dynamic graphs are simply static graphs where edges have time attributes Kazemi et al. [2020]. Representation learning approaches for dynamic graphs aim to learn how to effectively encode recurring structural and temporal patterns for node-level downstream tasks. For instance, Future Link Prediction (FLP) uses past interactions to predict future links, while Dynamic Node Classification (DNC) focuses on predicting labels of upcoming nodes based on impending interactions. While models based on Message-Passing Neural Networks (MPNN) Gilmer et al. [2017] have demonstrated impressive performance on encoding dynamic graphs Rossi et al. [2020], Wang et al. [2021], Jin et al. [2022], Luo and Li [2022], many approaches have notable limitations. Primarily, these methods often rely heavily on chronological training or use complex memory modules for predictions Kumar et al. [2019], Xu et al. [2020], Rossi et al. [2020], Wang et al. [2021], leading to significant computational overhead, especially for dynamic graphs with many edges. Additionally, the use of inefficient message-passing procedures can be problematic, and some

---

[*]Both authors contributed equally to the paper.

methods depend on computationally expensive random-walk-based algorithms Wang et al. [2021], Jin et al. [2022]. These methods often require heuristic feature engineering, which is specifically tailored for edge-level tasks.

Moreover, there is a growing consensus within the community that the message-passing paradigm is inherently constrained by the hard inductive biases imposed by the graph structure Kreuzer et al. [2021]. A central concern with conventional MPNNs revolves around the over-smoothing problem stemmed from the exponential growth of the model's computation graph Dwivedi and Bresson [2020]. This issue becomes pronounced when the model attempts to capture the higher-order long-range aspects of the graph structure. Over-smoothing hurts model expressiveness in MPNNs where the network depth grows in an attempt to increase expressiveness. However, the node embeddings tend to converge towards a constant uninformative representation. This serves as a reminder of the lack of flexibility observed in early recurrent neural networks used in Natural Language Processing (NLP), especially when encoding lengthy sentences or attempting to capture long-range dependencies within sequences Hochreiter and Schmidhuber [1997]. However, Transformers have mitigated these limitations in various data modalities Vaswani et al. [2017], Devlin et al. [2018], Liu et al. [2021], Dosovitskiy et al. [2020], Dwivedi and Bresson [2020]. Over-squashing is another problem that message-passing networks suffer from since the amount of local information aggregated repeatedly increases proportionally with the number of edges and nodes Hamilton [2020], Topping et al. [2021].

To address the aforementioned learning challenges on dynamic graphs, we propose Todyformer —a novel Graph Transformer model on dynamic graphs that unifies the local and global message-passing paradigms by introducing patchifying, tokenization, and encoding modules that collectively aim to improve model expressiveness through alleviating over-squashing and over-smoothing in a systematic manner. To mitigate the neighborhood explosion (i.e, over-squashing), we employ temporal-order-preserving patch generation, a mechanism that divides large dynamic graphs into smaller dynamic subgraphs. This approach breaks the larger context into smaller subgraphs suitable for local message-passing, instead of relying on the model to directly analyze the granular and abundant features of large dynamic graphs.

Moreover, we adopt a hybrid approach to successfully encode the long-term contextual information, where we use MPNNs for tasks they excel in, encoding local information, while transformers handle distant contextual dependencies. In other words, our proposed architecture adopts the concept of learnable structure-aware tokenization, reminiscent of the Vision Transformer (ViT) paradigm Dosovitskiy et al. [2020], to mitigate computational overhead. Considering the various contributions of this architecture, Todyformer dynamically alternates between encoding local and global contexts, particularly when capturing information for anchor nodes. This balances between the local and global computational workload and augments the model expressiveness through the successive stacking of the MPNN and Transformer modules.

2 Related Work

Representation learning for dynamic graphs: Recently, the application of machine learning to Continuous-Time Dynamic Graphs (CTDG) has drawn the attention of the graph community Kazemi et al. [2020]. RNN-based methods such as JODIE Divakaran and Mohan [2020], Know-E Trivedi et al. [2017], and DyRep Trivedi et al. [2019] typically update node embeddings sequentially as new edges arrive. TGAT Xu et al. [2020], akin to GraphSAGE Hamilton et al. [2017] and GAT Veličković et al. [2018], uses attention-based message-passing to aggregate messages from historical neighbors of an anchor node. TGN Rossi et al. [2020] augments the message-passing with an RNN-based memory module that stores the history of all nodes with a memory overhead. CAW Wang et al. [2021] and NeurTWs Jin et al. [2022] abandon the common message-passing paradigm by extracting temporal features from temporally-sampled causal walks. CAW operates directly within link streams and mandates the retention of the most recent links, eliminating the need for extensive memory storage. Moreover, Souza et al. [2022] investigates the theoretical underpinnings regarding the representational power of dynamic encoders based on message-passing and temporal random walks. DyG2Vec Alomrani et al. [2022] proposes an efficient attention-based encoder-decoder MPNN that leverages temporal edge encoding and window-based subgraph sampling to regularize the representation learning for task-agnostic node embeddings. GraphMixer Cong et al. [2023] simplifies the design of dynamic GNNs by employing fixed-time encoding functions and leveraging the MLP-Mixer architecture Tolstikhin et al. [2021].
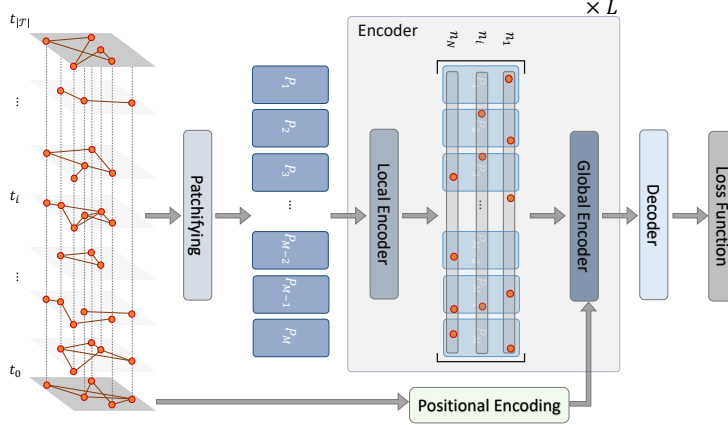
Figure 1: Illustration of Todyformer encoding-decoding architecture.

Graph Transformers: Transformers have been demonstrating remarkable efficacy across diverse data modalities Vaswani et al. [2017], Dosovitskiy et al. [2020]. The graph community has recently started to embrace them in various ways Dwivedi and Bresson [2020]. Graph-BERT Zhang et al. [2020] avoids message-passing by mixing up global and relative scales of positional encoding. Kreuzer et al. [2021] proposes a refined inductive bias for Graph Transformers by introducing a soft and learnable positional encoding (PE) rooted in the graph Laplacian domain, signifying a substantive stride in encoding low-level graph structural intricacies. Ying et al. [2021] is provably more powerful than 1-WL; it abandons Laplacian PE in favor of spatial and node centrality PEs. Subsequently, SAT Chen et al. [2022] argues that Transformers with PE do not necessarily capture structural properties. Therefore, the paper proposes applying GNNs to obtain initial node representations. Graph GPS Rampášek et al. [2022] provides a recipe to build scalable Graph Transformers, leveraging structural and positional encoding where MPNNs and Transformers are jointly utilized to address over-smoothing, similar to SAT. TokenGT Kim et al. [2022] demonstrates that standard Transformers, without graph-specific modifications, can yield promising results in graph learning. It treats nodes and edges as independent tokens and augments them with token-wise embeddings to capture the graph structure. He et al. [2023] adapts MLP-Mixer Tolstikhin et al. [2021] architectures to graphs, partitioning the input graph into patches, applying GNNs to each patch, and fusing their information while considering both node and patch PEs. While the literature adapts Transformers to static graphs, a lack of attention is eminent on dynamic graphs. In this work, we strive to shed light on such adaptation in a principled manner and reveal how dynamic graphs can naturally benefit from a unified local and global encoding paradigm.

3 Todyformer: Tokenized Dynamic Graph Transformer

We begin this section by presenting the problem formulation of this work. Next, we provide the methodological details of the Todyformer architecture along with its different modules.

Problem Formulation: A CTDG $\mathcal{G} = (\mathcal{V}, \mathcal{E}, \mathcal{X}^E, \mathcal{X}^v)$ with $N = |\mathcal{V}|$ nodes and $E = |\mathcal{E}|$ edges can be represented as a sequence of interactions $\mathcal{E} = \{e_1, e_2, \ldots, e_E\}$, where $\mathcal{X}^v \in \mathbb{R}^{N \times D^V}$ and $\mathcal{X}^E \in \mathbb{R}^{E \times D^E}$ are the node and edge features, respectively. D^V and D^E are the dimensions of the node and edge feature space, respectively. An edge $e_i = (u_i, v_i, t_i, m_i)$ links two nodes $u_i, v_i \in \mathcal{V}$ at a continuous timestamp $t_i \in \mathbb{R}$, where $m_i \in \mathcal{X}^E$ is an edge feature vector. Without loss of generality, we assume that the edges are undirected and ordered by time (i.e., $t_i \leq t_{i+1}$). A temporal sub-graph $\mathcal{G}_{ij}$ is defined as a set consisting of all the edges in the interval $[t_i, t_j]$, such that $\mathcal{E}_{ij} = \{e_k \mid t_i \leq t_k < t_j\}$. Any two nodes can interact multiple times throughout the time horizon; therefore, $\mathcal{G}$ is a multi-graph. Following DyG2Vec Alomrani et al. [2022], we adopt a window-based encoding paradigm for dynamic graphs to control representation learning and balance the trade-off between efficiency and accuracy according to the characteristics of the input data domain. The parameter W controls the size of the window for the input graph $\mathcal{G}_{ij}$, where $j = i + W$. For notation brevity, we assume the window mechanism is implicit from the context. Hence, we use $\mathcal{G}$ as the input graph unless explicit clarification is needed.
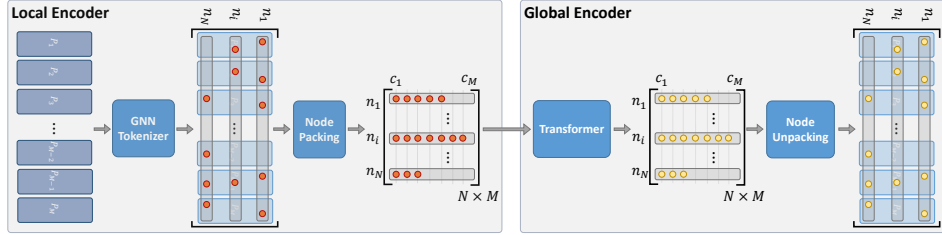
3

Figure 2: Schematic depiction of the computation flow in the local and global encoding modules, particularly highlighting node packing and unpacking modules in Todyformer.

Based on the downstream task, the objective is to learn the weight parameters θ and γ of a dynamic graph encoder f_θ and decoder g_γ respectively. f_θ projects the input graph $\mathcal{G}$ to the node embeddings $H \in \mathbb{R}^{N \times D^H}$, capturing temporal and structural dynamics for the nodes. Meanwhile, a decoder g_γ outputs the predictions given the node embeddings for the downstream task, enabling accurate future predictions based on past interactions. More specifically: $\mathrm{H} = \mathrm{f}_\theta(\mathcal{G})$, $Z = g_\gamma(H)$, Here, Z represents predictions for the ground-truth labels. In this work, we focus on common downstream tasks defined similarly to Alomrani et al. [2022] for training and evaluation: i) Future Link Prediction (FLP) and ii) Dynamic Node Classification (DNC).

3.1 Encoder Architecture

Todyformer consists of L blocks of encoding $f_\theta = \{(u^l, v^l)\}_{l=0}^L$ where $u = \{u^l\}_{l=0}^L$ and $v = \{v^l\}_{l=0}^L$ are the sets of local and global encoding modules, respectively. As illustrated in Figure 1, the encoding network of Todyformer benefits from an alternating architecture that alternates between local and global message-passing. The local encoding is structural and temporal, according to the learnable tokenizer, and the global encoding in this work is defined to be temporal. We leave the structural and temporal global encoding for future work. In the following, we define each encoding module in more detail.

3.2 Patch Generation

Inspired by Dosovitskiy et al. [2020], Todyformer begins by partitioning a graph into M subgraphs, each containing an equal number of edges. This partitioning is performed based on the timestamp associated with each edge. Specifically, the patchifier p evenly segments the input graph $\mathcal{G}$ with $\mathcal{E} = \{e_1, e_2, \ldots, e_E\}$ edges into M non-overlapping subgraphs of equal size, referred to as patches. More concretely:

$$\mathcal{P} = p(\mathcal{G}; M) \tag{1}$$

where $\mathcal{P} = \{\mathcal{G}_m \,|\, m \in \{1, 2, ..., \frac{E}{M}\}\}$ and the m-th graph, denoted as $\mathcal{G}_m$, consists of edges with indices in the range $\{(m-1)\frac{E}{M}+1, \cdots, m\frac{E}{M}\}$. Partitioning the input graph into M disjoint subgraphs helps message-passing to be completely separated within each patch. Additionally, M manages the trade-off between alleviating over-squashing and maintaining the tokenizer's expressiveness. Through ablation studies, we empirically reveal how different datasets react to various M values.

3.3 Local Encoding: Structure-Aware Tokenization

Local encoding $u^l = (s^l, c)$ contains two modules: the tokenization s^l and the packing c modules. The former handles local tokenization, and the latter packs tokens into a sequential data structure that will be consumed by the global encoder.

Structure-Aware Tokenization: Following the recent trend in Graph Transformers, where tokenization is structure-aware, local encoding in Todyformer utilizes a dynamic GNN to map the input node embeddings to the latent embeddings that a Transformer will process later on. It should be noted that the tokenizer has learnable parameters to encode both structural and temporal patterns in the

4

patches. Without loss of generality, we use DyG2Vec Alomrani et al. [2022] as a powerful attentive message-passing model to locally encode input features into semantically meaningful node tokens.

$$\mathcal{H}^l = s^l(\acute{\mathcal{H}}^{l-1}) \tag{2}$$

where $\mathcal{H}^l = \{H_i^l\}_{i=0}^{M-1}$ is the set of node embeddings H_i for M different patches, and $\acute{\mathcal{H}}^{l-1}$ is the set of node embeddings computed by the previous block. As illustrated in Figure 1, the output of one block from the global encoder is transferred as the input into the local encoder of the subsequent block. It should be noted that $\acute{\mathcal{H}}^0 = \mathcal{X}$ for the first layer, where $\mathcal{X} = \{X_i\}_{i=0}^{M-1}$ is the set of node features for all patches.

Packing: Once the node features are locally encoded into node tokens, the next step is to pack the set of node embeddings $\mathcal{H}^l$ into the standard format required by Transformers. Since a node may appear in multiple patches, to collect all the node embeddings for a particular node across the patches, a node-packing module c is utilized. This module collects the embeddings of all nodes across the patches and arranges them in a sequential data format as follows:

$$H^l = c(\mathcal{H}^l, \mathcal{P}) \tag{3}$$

where $H^l \in \mathbb{R}^{N \times M \times D^H}$ such that N is the number of nodes in the input graph $\mathcal{G}$, M is the total number of patches, and D^H is the dimension of the embedding space. The module c uses $\mathcal{P}$ to figure out which patches a node belongs to. Consequently, the output of the local encoding module is structured in a tensor that can be easily consumed by a Transformer. The computation flow in the local encoder is shown in Figure 2. Since nodes may have interactions for a variable number of times in the input graph, it is necessary to pad the short sequences with the $[\text{MASK}]$ tokens at the end. Then, the mini-batch of sequences can be easily packed into a dense tensor and fed as input to Transformers.

3.4 Global Encoding

The packed node tokens will be fed into the global encoding module to perform long-range message-passing beyond the local context of the input patches. Therefore, Todyformer not only maximizes the parametric capacity of MPNNs to encode local context but also leverages the long-range capacities of Transformers to improve the model expressiveness. The global encoder $v^l = (o^l, r^l, n^l)$ consists of the positional encoder o^l, Transformer r^l, and unpacking module n^l according to the details provided in the following.

Positional Encoding: Transformers are aware of the ordering in the input sequences through positional encoding. Various systematic approaches have been investigated in the literature for the sake of improved expressiveness [Dwivedi and Bresson, 2020, Kreuzer et al., 2021]. Once the structural and temporal features are locally mapped into node tokens, and the sequential input H^l is packed at layer l, positional encoding is needed to inform the Transformer of the temporal ordering of the node tokens on a global scale. The positional encoding in Todyformer is defined based on the notion of the position and the encoding function. The position can be explicitly defined as the global edge index of a node upon an interaction at a timestamp or implicitly defined as the patch or occurrence indices. The encoding function can be a linear or sinusoidal mapping. The PE is fused into the packed node embeddings through the addition modulation, as follows:

$$H^l = H^l + P, \qquad P = o(\mathcal{P}) \in \mathbb{R}^{N \times M \times D^H} \tag{4}$$

Transformer: The global encoding updates node embeddings through a dot-product Multi-head Self-Attention (MSA) Transformer architecture as follows:

$$\bar{H}^l = r^l(H^l), \qquad r^l = \texttt{Transformer}(Q, K, V) = softmax\big(\frac{QK^T}{\sqrt{d_k}}\big)V \tag{5}$$

where $Q = H^l W_q \in \mathbb{R}^{N \times D^k}$, $K = H^l W_k \in \mathbb{R}^{N \times D^k}$, and $V = H^l W_v \in \mathbb{R}^{N \times D^v}$ are the query, key, and value, respectively, and $W_q, W_k \in \mathbb{R}^{D^H \times D^k}$ and $W_v \in \mathbb{R}^{D^H \times D^v}$ are learnable matrices.

Table 1: Future Link Prediction Performance in AP (Mean ± Std) on the test set.

Setting	Model	MOOC	LastFM	Enron	UCI	SocialEvol.
Transductive	JODIE	0.797 ± 0.01	0.691 ± 0.010	0.785 ± 0.020	0.869 ± 0.010	0.847 ± 0.014
	DyRep	0.840 ± 0.004	0.683 ± 0.033	0.795 ± 0.042	0.524 ± 0.076	0.885 ± 0.004
	TGAT	0.793 ± 0.006	0.633 ± 0.002	0.637 ± 0.002	0.835 ± 0.003	0.631 ± 0.001
	TGN	0.911 ± 0.010	0.743 ± 0.030	0.866 ± 0.006	0.843 ± 0.090	0.966 ± 0.001
	CaW	0.940 ± 0.014	$0.903 \pm 1e{-}4$	0.970 ± 0.001	0.939 ± 0.008	$0.947 \pm 1e{-}4$
	NAT	0.874 ± 0.004	$0.859 \pm 1e{-}4$	0.924 ± 0.001	0.944 ± 0.002	0.944 ± 0.010
	GraphMixer	0.835 ± 0.001	0.862 ± 0.003	0.824 ± 0.001	0.932 ± 0.006	$0.935 \pm 3e{-}4$
	Dygformer	0.892 ± 0.005	0.901 ± 0.003	0.926 ± 0.001	0.959 ± 0.001	$0.952 \pm 2e{-}4$
	DyG2Vec	0.980 ± 0.002	$0.960 \pm 1e{-}4$	0.991 ± 0.001	0.988 ± 0.007	$0.987 \pm 2e{-}4$
	Todyformer	$\mathbf{0.992 \pm 7e{-}4}$	$\mathbf{0.976 \pm 3e{-}4}$	$\mathbf{0.995 \pm 6e{-}4}$	$\mathbf{0.994 \pm 4e{-}4}$	$\mathbf{0.992 \pm 1e{-}4}$
Inductive	JODIE	0.707 ± 0.029	0.865 ± 0.03	0.747 ± 0.041	0.753 ± 0.011	0.791 ± 0.031
	DyRep	0.723 ± 0.009	0.869 ± 0.015	0.666 ± 0.059	0.437 ± 0.021	$0.904 \pm 3e{-}4$
	TGAT	0.805 ± 0.006	0.644 ± 0.002	0.693 ± 0.004	0.820 ± 0.005	0.632 ± 0.005
	TGN	0.855 ± 0.014	0.789 ± 0.050	0.746 ± 0.013	0.791 ± 0.057	0.904 ± 0.023
	CaW	0.933 ± 0.014	0.890 ± 0.001	0.962 ± 0.001	0.931 ± 0.002	$0.950 \pm 1e{-}4$
	NAT	$0.832 \pm 1e{-}4$	0.878 ± 0.003	0.949 ± 0.010	0.926 ± 0.010	0.952 ± 0.006
	GraphMixer	0.814 ± 0.002	0.821 ± 0.004	0.758 ± 0.004	0.911 ± 0.004	$0.918 \pm 6e{-}4$
	Dygformer	0.869 ± 0.004	$0.942 \pm 9e{-}4$	0.897 ± 0.003	0.945 ± 0.001	$0.931 \pm 4e{-}4$
	DyG2Vec	0.938 ± 0.010	0.979 ± 0.006	0.987 ± 0.004	0.976 ± 0.002	0.978 ± 0.010
	Todyformer	$\mathbf{0.948 \pm 0.009}$	$\mathbf{0.981 \pm 0.005}$	$\mathbf{0.989 \pm 8e{-}4}$	$\mathbf{0.983 \pm 0.002}$	$\mathbf{0.9821 \pm 0.005}$

We apply an attention mask to enforce directed connectivity between node tokens through time, where a node token from the past is connected to all others in the future. The Transformer module is expected to learn temporal inductive biases from the context on how to deploy attention on recent interactions versus early ones.

Unpacking: For intermediate blocks, the unpacking module n^l is necessary to transform the packed, unstructured sequential node embeddings back into the structured counterparts that can be processed alternately by the local encoder of the next block. It is worth mentioning that the last block L does not require an unpacking module. Instead, a readout function e is defined to return the final node embeddings consumed by the task-specific decoding head:

$$\vec{\mathcal{H}}^l = n^l(\bar{H}^l), \qquad \bar{H}^L = e(\bar{H}^{L-1}) \in \mathbb{R}^{N \times D^H} \tag{6}$$

where $\vec{\mathcal{H}}^l = \{\bar{H}_i^l\}_{i=0}^{M-1}$ is the set of node embeddings $\bar{H}_i$ for M different patches, e is the readout function, and D^H is the dimension of the output node embeddings. The readout function is defined to be a MAX, MEAN, or LAST pooling layer.

3.5 Improving Over-Smoothing by Alternating Architecture

Over-smoothing is a critical problem in graph representation learning, where MPNNs fall short in encoding long-range dependencies beyond a few layers of message-passing. This issue is magnified in dynamic graphs when temporal long-range dependencies intersect with structural patterns. MPNNs typically fall into the over-smoothing regime beyond a few layers (e.g., 3), which may not be sufficient to capture long-range temporal dynamics. We propose to address this problem by letting the Transformer widen up the temporal contextual node-wise scope beyond a few hops in an alternating manner. For instance, a 3-layer MPNN encoder can reach patterns up to 9 hops away in Todyformer.

4 Experimental Evaluation

In this section, we evaluate the generalization performance of Todyformer through a rigorous empirical assessment, spanning a wide range of benchmark datasets across the downstream tasks. First, the experimental setup is explained and a comparison with state-of-the-art (SoTA) on dynamic graphs is given. Next, the quantitative results are presented. Later, in-depth comparative analysis and ablation studies are provided to further highlight the role of the design choices in this work.

4.1 Experimental Setup

Baselines: The performance of Todyformer is compared with a wide spectrum of dynamic graph encoders, ranging from random-walk based to attentive memory-based approaches: DyRep [Trivedi

Table 2: Future Link Prediction performance on the test set of TGBL datasets measured using Mean Reciprocal Rank (MRR). The baseline results are directly taken from Huang et al. [2023].

Model	Wiki	Review	Coin	Comment	Flight	Avg. Rank ↓
Dyrep	0.366 ± 0.014	0.367 ± 0.013	0.452 ± 0.046	0.289 ± 0.033	0.556 ± 0.014	4.4
TGN	0.721 ± 0.004	$\mathbf{0.532 \pm 0.020}$	0.586 ± 0.037	0.379 ± 0.021	0.705 ± 0.020	2
CAW	$\mathbf{0.791 \pm 0.015}$	0.194 ± 0.004	OOM	OOM	OOM	4.4
TCL	0.712 ± 0.007	0.200 ± 0.010	OOM	OOM	OOM	4.8
GraphMixer	0.701 ± 0.014	0.514 ± 0.020	OOM	OOM	OOM	4.4
EdgeBank	0.641	0.0836	0.1494	0.364	0.580	4.6
Todyformer	0.7738 ± 0.004	$0.5104 \pm 86e{-}4$	$\mathbf{0.689 \pm 18e{-}4}$	$\mathbf{0.762 \pm 98e{-}4}$	$\mathbf{0.777 \pm 0.014}$	**1.6**

et al., 2019], JODIE [Kumar et al., 2019], TGAT [Xu et al., 2020], TGN [Rossi et al., 2020], CaW [Wang et al., 2021], NAT Luo and Li [2022], and DyG2Vec Alomrani et al. [2022]. CAW samples temporal random walks and learns temporal motifs by counting node occurrences in each walk. NAT constructs temporal node representations using a cache that stores a limited set of historical interactions for each node. DyG2Vec introduces a window-based MPNN that attentively aggregates messages in a window of recent interactions. Recently, GraphMixer Cong et al. [2023] as a simple yet effective MLP-Mixer-based dynamic graph encoder. Dygformer Yu et al. [2023] also presents a Transformer architecture that encodes the one-hop node neighborhoods.

Downstream Tasks: We evaluate all of the models on both FLP and DNC. In FLP, the goal is to predict the probability of future edges occurring given the source and destination nodes, and the timestamp. For each positive edge, we sample a negative edge that the model is trained to predict as negative. The DNC task involves predicting the ground-truth label of the source node of a future interaction. Both tasks are trained using binary cross entropy loss function. For FLP, we evaluate all models on the transductive and inductive settings. The latter is a more challenging setting where a model makes a prediction on unseen nodes. The Average Precision (AP) and the Area Under the Curve (AUC) metrics are reported for the FLP and DNC tasks respectively. DNC is evaluated on AUC due to the class imbalance issue.

Datasets: In the first set of experiments, we use 5 real-world datasets for FLP: MOOC, and LastFM [Kumar et al., 2019]; SocialEvolution, Enron, and UCI [Wang et al., 2021]. Three real-world datasets including Wikipedia, Reddit, MOOC [Kumar et al., 2019] are used for DNC as well. These datasets span a wide range of the number of nodes and interactions, timestamp ranges, and repetition ratios. The dataset statistics are presented in Appendix 6.1 We perform the same 70%-15%-15% chronological split for all datasets as in [Wang et al., 2021]. The datasets are split differently under two settings: Transductive and Inductive. All the benchmark datasets are publicly available. We follow similar experimental setups to Alomrani et al. [2022], Wang et al. [2021] on these datasets to split into training, validation, and test sets under the transductive and inductive settings.

In the second set of experiments, we evaluate Todyformer on the Temporal Graph Benchmark for link prediction datasets (TGBL) Huang et al. [2023]. The goal is to target large-scale and real-world experimental setups with a higher number of negative samples generated based on two policies: random and historical. The deliberate inclusion of such negative edges aims to address the substantial bias inherent in negative sampling techniques, which can significantly affect model performance inference. Among the 5 datasets, 3 are extra-large-scale where model training on a regular setup may take weeks of processing. We follow the experimental setups similar to Huang et al. [2023] to evaluate our model on TGBL (e.g., number of trials or negative sampling).

Model Hyperparameters: Todyformer has a large number of hyperparameters to investigate. There are common design choices such as activation layers, normalization layers, and skip connections that we assumed the results are less sensitive to in order to dial down the total number of trials. We chose $L = 3$ for the number of blocks in the encoder. The GNN and Transformers have 3 and 2 layers respectively. The neighbor sampler in the local encoder uniformly samples $(64, 1, 1)$ number of neighbors for 3 hops. The model employs uniform sampling within the window instead of selecting the latest N neighbors of a node [Xu et al., 2020, Rossi et al., 2020]. For the DNC task, following prior work Rossi et al. [2020], the decoder is trained on top of the frozen encoder pre-trained on FLP.

4.2 Experimental Results

Future Link Prediction: We present a comparative analysis of AP scores on the test set for future link prediction (both transductive and inductive) across several baselines in Table 1. Notably, a substantial performance gap is evident on the transductive setting, with Todyformer outperforming the second-best model by margins exceeding 1.2%, 1.6%, 0.6%, and 0.5% on the MOOC, LastFM, UCI, and SocialEvolve datasets, respectively. Despite the large scale of SocialEvolve dataset with around 2 million edges, our model achieves SoTA performance on this dataset. This observation

Table 3: Dynamic Node Classification performance in AUC (Mean ± Std) on the test set. Avg. Rank reports the mean rank of a method across all datasets.

Model	Wikipedia	Reddit	MOOC	Avg. Rank ↓
TGAT	0.800 ± 0.010	$\textbf{0.664} \pm \textbf{0.009}$	0.673 ± 0.006	3.6
JODIE	0.843 ± 0.003	0.566 ± 0.016	0.672 ± 0.002	4.6
Dyrep	$\textbf{0.873} \pm \textbf{0.002}$	0.633 ± 0.008	0.661 ± 0.012	4
TGN	0.828 ± 0.004	0.655 ± 0.009	0.674 ± 0.007	3.3
DyG2Vec	0.824 ± 0.050	0.649 ± 0.020	$\textbf{0.785} \pm \textbf{0.005}$	3.3
Todyformer	$\underline{0.861} \pm 0.017$	$\underline{0.656} \pm 0.005$	$\underline{0.745} \pm 0.009$	**2**

reinforces the conclusions drawn in Xu et al. [2020], emphasizing the pivotal role played by recent temporal links in the future link prediction task. Within the inductive settings, Todyformer continues to exhibit superior performance across all datasets. The challenge posed by the prediction of links over unseen nodes impacts the overall performance of most methods. However, Todyformer consistently outperforms the baselines' results on all datasets. These empirical results support the hypothesis that model expressiveness has been improved significantly while increasing the generalization under the two experimental settings. Additionally, Todyformer outperforms the two latest SoTA methods namely GraphMixer Cong et al. [2023] and Dygformer Yu et al. [2023]. The results further validate that the dynamic graphs require encoding of the long-range dependencies that cannot be simply represented by the short-range one-hop neighborhoods. This further verifies that multi-scale encoders like Todyformer are capable of learning the inductive biases across various domains.

Additionally, the performance of Todyformer on 2 small and 3 large TGBL datasets are presented in Table 2. On extra-large TGBL datasets (Coin, Comment, and Flight), Todyformer outperforms SoTA with significant margins, exceeding 11%, 39%, and 7% respectively. This interestingly supports the hypothesis behind the expressive power of the proposed model to scale up to the data domains with extensive long-range interactions. In the case of smaller datasets like TGBL-Wiki and TGBL-Review, our approach attains the second and third positions in the ranking respectively. It should be noted that hyperparameter search has not been exhausted during experimental evaluation. The average ranking reveals that Todyformer is ranked first, followed by TGN in second place on this challenging experimental setup.

Dynamic Node classification: Todyformer has undergone extensive evaluation across three datasets dedicated to node classification. In these datasets, dynamic sparse labels are associated with nodes within a defined time horizon after interactions. This particular task grapples with a substantial imbalanced classification challenge. Table 3 presents AUC metric, known for its robustness toward class imbalance, across various methods on the three datasets. Notably, Todyformer demonstrates remarkable performance, trailing the best by only 4% in the MOOC dataset and 1% in both the Reddit and Wikipedia datasets. Across all datasets, Todyformer consistently secures the second-best position. However, it's important to acknowledge that no model exhibits consistent improvement across all datasets, primarily due to the presence of data imbalance issues inherent in anomaly detection tasks Ranshous et al. [2015]. To establish the ultimate best model, we have computed the average ranks of various methods. Todyformer emerges as the top performer with an impressive rank of 2 validating the overall performance improvement.

Ablation Studies and Sensitivity Analysis: In Appendix 6.4, We conducted experiments to assess the sensitivity of the major hyperparameters across various parameters and datasets.

5   Conclusion

We propose Todyformer, a tokenized graph Transformer for dynamic graphs where over-smoothing and over-squashing are empirically improved through a local and global encoding architecture. We present how to adapt the best practices of Transformers in various data domains (e.g. Computer Vision) to dynamic graphs in a principled manner. Primary novel components are patch generation, structure-aware tokenization using typical MPNNs that locally encode neighborhoods, and the utilization of Transformers to aggregate global context in an alternating fashion. The consistent experimental gains across different experimental settings empirically support the hypothesis that the SoTA dynamic graph encoders severely suffer from over-squashing and over-smoothing phenomena, especially on real-world large-scale datasets introduced in TGBL. We hope Todyformer sheds light on the underlying aspects of dynamic graphs and opens up the door for further principled investigation on dynamic graph transformers.

References

Seyed Mehran Kazemi, Rishab Goel, Kshitij Jain, Ivan Kobyzev, Akshay Sethi, Peter Forsyth, and Pascal Poupart. Representation learning for dynamic graphs: A survey. *Journal of Machine Learning Research*, 2020.

Justin Gilmer, Samuel S Schoenholz, Patrick F Riley, Oriol Vinyals, and George E Dahl. Neural message passing for quantum chemistry. In *International conference on machine learning*. PMLR, 2017.

Emanuele Rossi, Ben Chamberlain, Fabrizio Frasca, Davide Eynard, Federico Monti, and Michael Bronstein. Temporal graph networks for deep learning on dynamic graphs. In *ICML Workshop on Graph Representation Learning*, 2020.

Yanbang Wang, Yen-Yu Chang, Yunyu Liu, Jure Leskovec, and Pan Li. Inductive representation learning in temporal networks via causal anonymous walks. In *Proc. Int. Conf. on Learning Representations*, 2021.

Ming Jin, Yuan-Fang Li, and Shirui Pan. Neural temporal walks: Motif-aware representation learning on continuous-time dynamic graphs. In *Thirty-Sixth Conference on Neural Information Processing Systems*, 2022.

Yuhong Luo and Pan Li. Neighborhood-aware scalable temporal network representation learning. In *The First Learning on Graphs Conference*, 2022.

Srijan Kumar, Xikun Zhang, and Jure Leskovec. Predicting dynamic embedding trajectory in temporal interaction networks. In *Proc. Int. Conf. on Knowledge Discovery & Data Mining*, 2019.

Da Xu, Chuanwei Ruan, Evren Korpeoglu, Sushant Kumar, and Kannan Achan. Inductive representation learning on temporal graphs. *Proc. Int. Conf. on Representation Learning*, 2020.

Devin Kreuzer, Dominique Beaini, Will Hamilton, Vincent Létourneau, and Prudencio Tossou. Rethinking graph transformers with spectral attention. *Advances in Neural Information Processing Systems*, 34:21618–21629, 2021.

Vijay Prakash Dwivedi and Xavier Bresson. A generalization of transformer networks to graphs. *arXiv preprint arXiv:2012.09699*, 2020.

Sepp Hochreiter and Jürgen Schmidhuber. Long short-term memory. *Neural computation*, 9(8):1735–1780, 1997.

Ashish Vaswani, Noam Shazeer, Niki Parmar, Jakob Uszkoreit, Llion Jones, Aidan N Gomez, Łukasz Kaiser, and Illia Polosukhin. Attention is all you need. *Advances in neural information processing systems*, 30, 2017.

Jacob Devlin, Ming-Wei Chang, Kenton Lee, and Kristina Toutanova. Bert: Pre-training of deep bidirectional transformers for language understanding. *arXiv preprint arXiv:1810.04805*, 2018.

Ze Liu, Yutong Lin, Yue Cao, Han Hu, Yixuan Wei, Zheng Zhang, Stephen Lin, and Baining Guo. Swin transformer: Hierarchical vision transformer using shifted windows. In *Proceedings of the IEEE/CVF international conference on computer vision*, pages 10012–10022, 2021.

Alexey Dosovitskiy, Lucas Beyer, Alexander Kolesnikov, Dirk Weissenborn, Xiaohua Zhai, Thomas Unterthiner, Mostafa Dehghani, Matthias Minderer, Georg Heigold, Sylvain Gelly, et al. An image is worth 16x16 words: Transformers for image recognition at scale. *arXiv preprint arXiv:2010.11929*, 2020.

William L Hamilton. *Graph representation learning*. Morgan & Claypool Publishers, 2020.

Jake Topping, Francesco Di Giovanni, Benjamin Paul Chamberlain, Xiaowen Dong, and Michael M Bronstein. Understanding over-squashing and bottlenecks on graphs via curvature. *arXiv preprint arXiv:2111.14522*, 2021.

Aswathy Divakaran and Anuraj Mohan. Temporal link prediction: A survey. *New Generation Computing*, 38(1): 213–258, 2020.

Rakshit Trivedi, Hanjun Dai, Yichen Wang, and Le Song. Know-evolve: Deep temporal reasoning for dynamic knowledge graphs. In *Proc. Int. Conf. on Machine Learning*, pages 3462–3471. PMLR, 2017.

Rakshit Trivedi, Mehrdad Farajtabar, Prasenjeet Biswal, and Hongyuan Zha. Dyrep: Learning representations over dynamic graphs. In *Proc. Int. Conf. on Learning Representations*, 2019.

William L. Hamilton, Zhitao Ying, and Jure Leskovec. Inductive representation learning on large graphs. In *Proc. Adv. Neural Inf. Proc. Systems*, 2017.

Petar Veličković, Guillem Cucurull, Arantxa Casanova, Adriana Romero, Pietro Liò, and Yoshua Bengio. Graph Attention Networks. In *ICLR*, 2018.

Amauri Souza, Diego Mesquita, Samuel Kaski, and Vikas Garg. Provably expressive temporal graph networks. *Advances in Neural Information Processing Systems*, 35:32257–32269, 2022.

Mohammad Ali Alomrani, Mahdi Biparva, Yingxue Zhang, and Mark Coates. Dyg2vec: Representation learning for dynamic graphs with self-supervision. *arXiv preprint arXiv:2210.16906*, 2022.

Weilin Cong, Si Zhang, Jian Kang, Baichuan Yuan, Hao Wu, Xin Zhou, Hanghang Tong, and Mehrdad Mahdavi. Do we really need complicated model architectures for temporal networks? *arXiv preprint arXiv:2302.11636*, 2023.

Ilya O Tolstikhin, Neil Houlsby, Alexander Kolesnikov, Lucas Beyer, Xiaohua Zhai, Thomas Unterthiner, Jessica Yung, Andreas Steiner, Daniel Keysers, Jakob Uszkoreit, et al. Mlp-mixer: An all-mlp architecture for vision. *Advances in neural information processing systems*, 34:24261–24272, 2021.

Jiawei Zhang, Haopeng Zhang, Congying Xia, and Li Sun. Graph-bert: Only attention is needed for learning graph representations. *arXiv preprint arXiv:2001.05140*, 2020.

Chengxuan Ying, Tianle Cai, Shengjie Luo, Shuxin Zheng, Guolin Ke, Di He, Yanming Shen, and Tie-Yan Liu. Do transformers really perform badly for graph representation? *Advances in Neural Information Processing Systems*, 34:28877–28888, 2021.

Dexiong Chen, Leslie O'Bray, and Karsten Borgwardt. Structure-aware transformer for graph representation learning. In *International Conference on Machine Learning*, pages 3469–3489. PMLR, 2022.

Ladislav Rampášek, Michael Galkin, Vijay Prakash Dwivedi, Anh Tuan Luu, Guy Wolf, and Dominique Beaini. Recipe for a general, powerful, scalable graph transformer. *Advances in Neural Information Processing Systems*, 35:14501–14515, 2022.

Jinwoo Kim, Dat Nguyen, Seonwoo Min, Sungjun Cho, Moontae Lee, Honglak Lee, and Seunghoon Hong. Pure transformers are powerful graph learners. *Advances in Neural Information Processing Systems*, 35: 14582–14595, 2022.

Xiaoxin He, Bryan Hooi, Thomas Laurent, Adam Perold, Yann LeCun, and Xavier Bresson. A generalization of vit/mlp-mixer to graphs. In *International Conference on Machine Learning*, pages 12724–12745. PMLR, 2023.

Le Yu, Leilei Sun, Bowen Du, and Weifeng Lv. Towards better dynamic graph learning: New architecture and unified library. *arXiv preprint arXiv:2303.13047*, 2023.

Shenyang Huang, Farimah Poursafaei, Jacob Danovitch, Matthias Fey, Weihua Hu, Emanuele Rossi, Jure Leskovec, Michael Bronstein, Guillaume Rabusseau, and Reihaneh Rabbany. Temporal graph benchmark for machine learning on temporal graphs. *arXiv preprint arXiv:2307.01026*, 2023.

Stephen Ranshous, Shitian Shen, Danai Koutra, Steve Harenberg, Christos Faloutsos, and Nagiza F. Samatova. Anomaly detection in dynamic networks: a survey. *WIREs Computational Statistics*, 7(3):223–247, 2015.

Farimah Poursafaei, Shenyang Huang, Kellin Pelrine, and Reihaneh Rabbany. Towards better evaluation for dynamic link prediction. *Advances in Neural Information Processing Systems*, 35:32928–32941, 2022.

Seyed Mehran Kazemi, Rishab Goel, Sepehr Eghbali, Janahan Ramanan, Jaspreet Sahota, Sanjay Thakur, Stella Wu, Cathal Smyth, Pascal Poupart, and Marcus Brubaker. Time2vec: Learning a vector representation of time. *arXiv preprint arXiv:1907.05321*, 2019.

6 Supplementary Material

6.1 Dataset Statistics

In this section, we provide an overview of the statistics pertaining to two distinct sets of datasets utilized for the tasks of Future Link Prediction (FLP) and Dynamic Node Classification (DNC). The initial set, detailed in Table 4, presents information regarding the number of nodes, edges, and unique edges across seven datasets featured in Table 1 and Table 3. For these three datasets, namely Reddit, Wikipedia, and MOOC, all edge features have been incorporated, where applicable. Furthermore, within this table, the last column represents the percentage of Repetitive Edges, which signifies the proportion of edges that occur more than once within the dynamic graph.

Table 4: Dynamic Graph Datasets. **% Repetitive Edges**: % of edges which appear more than once in the dynamic graph.

Dataset	# Nodes	# Edges	# Unique Edges	Edge Features	Node Labels	Bipartite	% Repetitive Edges
Reddit	11,000	672,447	78,516	✓	✓	✓	54%
Wikipedia	9,227	157,474	18,257	✓	✓	✓	48%
MOOC	7,144	411,749	178,443	✓	✓	✓	53%
LastFM	1980	1,293,103	154,993			✓	68%
UCI	1899	59,835	13838			✓	62%
Enron	184	125,235	2215				92%
SocialEvolution	74	2,099,519	2506				97%

6.1.1 TGB dataset

In this section, we present the characteristics of datasets as proposed by the Dynamic Graph Encoder Leaderboard Huang et al. [2023]. Similar to previous benchmark datasets, we have conducted comparisons regarding the number of nodes, edges, and type of graphs. Additionally, we report the Number of Steps and the Surprise Index, as defined in Poursafaei et al. [2022], which illustrates the ratio of test edges that were not observed during the training phase.

Table 5: Statistics of TGBL Dynamic Graph Datasets

Dataset	# Nodes	# Edges	# Steps	Edge Features	Bipartite	Surprise Index Poursafaei et al. [2022]
Wiki	9,227	157,474	152,757	✓	✓	0.108
Review	352,637	4,873,540	6,865	✓	✓	0.987
Coin	638,486	22,809,486	1,295,720	✓		0.120
Comment	994,790	44,314,507	30,998,030	✓		0.823
Flight	18143	67,169,570	1,385	✓		0.024

6.2 Implementation details

In this section, we elucidate the intricacies of our implementation, providing a comprehensive overview of the specific parameters our model accommodates during hyperparameter optimization. Subsequently, we delve into a discussion of the optimal configurations and setups that yield the best performance for our proposed architecture.

Furthermore, in addition to an in-depth discussion of the baselines incorporated into our paper, we also offer a comprehensive overview of the respective hyperparameter configurations in this section. We are confident that with the open-sourcing of our code upon acceptance and the thorough descriptions of our model and baseline methodologies presented in the paper, our work is fully reproducible.

6.2.1 Evaluation Protocol

Transductive Setup: Under the transductive setting, a dataset is split normally by time, i.e., the model is trained on the first 70% of links, validated on $\%15$ and tested on the rest.

Inductive Setup: In the inductive setting, we strive to test the model's prediction performance on edges with unseen nodes. Therefore, following [Wang et al., 2021], we randomly assign 10% of the nodes to the validation and test sets and remove any interactions involving them in the training set.

Additionally, to ensure an inductive setting, we remove any interactions not involving these nodes from the test set.

6.2.2 Loss Function

As previously discussed in the main body of this paper, we focus on two specific downstream tasks: Future Link Prediction (FLP) and Dynamic Node Classification (DNC). For the former, we employ the binary cross-entropy loss, while for the latter, our model is trained through the minimization of the cross-entropy loss function. The formula for the binary cross-entropy loss is presented below:

$$H(y, \hat{y}) = -(y \cdot \log(\hat{y}) + (1 - y) \cdot \log(1 - \hat{y})) \tag{7}$$

where $y \in \{0, 1\}$ is the true label, and $\hat{y}$ is the predicted probability that the instance belongs to class 1. Moreover, the formulation of the cross-entropy loss is as follows:

$$H(y, \hat{y}) = -\sum_i y_i \cdot \log(\hat{y}_i) \tag{8}$$

where i represents the index over all classes, y_i is the true probability of the sample belonging to class i, encoded as a one-hot vector. It is 1 for the true class and 0 for all other classes. Finally, $\hat{y}_i$ is the predicted probability of the sample belonging to class i.

6.2.3 Best Hyperparameters for Benchmark datasets.

Table 6 displays the hyperparameters that have been subjected to experimentation and tuning for each dataset. For each parameter, a range of values has been tested as follows:

- Window Size (W): This parameter signifies the window length chosen for selecting the input subgraph based on edge timestamps. It falls within the range of $\in \{$ 16384, 32768 ,65536, 262144 $\}$.

- Number of Patches: This parameter indicates the count of equal and non-overlapping chunks for each input subgraph. It is the range of $\in \{8, 16, 32\}$.

- #Local Encoders: This parameter represents the number of local encoder layers within each block, and its value falls within the range of $\in \{1, 2\}$.

- Neighbor Sampling (NS) mode: $\in \{uniform, last\}$. In the case of a uniform Neighbor Sampler (NS), it uniformly selects samples from the 1-hop interactions of a given node. Conversely, in last mode, it samples from the most recent interactions.

- Anchor Node Mode: $\in \{GlobalTarget, LocalInput, LocalTarget\}$ depending on the mechanism of neighbor sampling we can sample from nodes within all patches (LocalInput), nodes within the next patch (LocalTarget), or global target nodes (GlobalTarget).

- Batch Size: $\in \{8, 16, 32, 64\}$

- Positional Encoding: $\in \{SineCosine, Time2Vec, Identity, Linear\}$

Dataset	Window Size (W)	Number of Patches	#Local Encoders	NS Mode	Anchor Node Mode	Batch Size
Reddit	262144	32	2	uniform	GlobalTarget	8
Wikipedia	65536	8	2	uniform	GlobalTarget	8
MOOC	65536	8	2	uniform	GlobalTarget	8
LastFM	262144	32	2	uniform	GlobalTarget	8
UCI	65536	8	2	uniform	GlobalTarget	8
Enron	65536	8	2	uniform	GlobalTarget	8
SocialEvolution	65536	8	2	uniform	GlobalTarget	8

Table 6: Best Parameters of the model pipeline after Hyperparameter search

SineCosine is utilized as the Positional Encoding (PE) method following the experiments conducted in Appendix 6.4.1.

Selecting Best Checkpoint: Throughout all experiments, the models undergo training for a duration of 100 epochs, with the best checkpoints selected for testing based on their validation Average Precision (AP) performance.

6.2.4 Best Hyperparameters for TGBL dataset

In this section, we present the optimal hyperparameters used in our architecture design for each TGBL dataset. We conducted hyperparameter tuning for all TGBL datasets; however, due to time constraints, we explored a more limited set of parameters for the large-scale dataset. Despite Todyformer outperforming its counterparts on these datasets, there remains potential for further improvement through an extensive hyperparameter search.

Dataset	Window Size (W)	Number of Patches	First-hop NS size	NS Mode	Anchor Node Mode	Batch Size
TGBWiki	262144	32	256	uniform	GlobalTarget	32
TGBReview	262144	32	64	uniform	GlobalTarget	64
TGBComment	65536	8	64	uniform	GlobalTarget	256
TGBCOin	65536	8	64	uniform	GlobalTarget	96
TGBFlight	65536	8	64	uniform	GlobalTarget	128

Table 7: Optimal Window size W for downstream training.

6.3 More Experimental Result

In this section, we present the additional experiments conducted and provide an analysis of the derived results and conclusions.

6.3.1 FLP result on Benchmark Datasets

Table 8 is an extension of Table 1, now incorporating the Wikipedia and Reddit datasets. Notably, for these two datasets, Todyformer attains the highest test Average Precision (AP) score in the Transductive setup. However, it secures the second-best and third-best positions in the Inductive setup for these Wikipedia and Reddit respectively. While the model does not attain the top position on these two datasets for inductive setup, its performance is only marginally below that of state-of-the-art (SOTA) models, which have previously achieved accuracy levels exceeding 99% Average Precision (AP).

Table 8: Future link Prediction Performance in AP (Mean $\pm$ Std). **Bold** font and <u>ul</u> font represent first- and second-best performance respectively.

Setting	Model	Wikipedia	Reddit	MOOC	LastFM	Enron	UCI	SocialEvol.
Transductive	JODIE	0.956 ± 0.002	0.979 ± 0.001	0.797 ± 0.01	0.691 ± 0.010	0.785 ± 0.020	0.869 ± 0.010	0.847 ± 0.014
	DyRep	0.955 ± 0.004	$0.981 \pm 1e{-}4$	0.840 ± 0.004	0.683 ± 0.033	0.795 ± 0.042	0.524 ± 0.076	0.885 ± 0.004
	TGAT	0.968 ± 0.001	$0.986 \pm 3e{-}4$	0.793 ± 0.006	0.633 ± 0.002	0.637 ± 0.002	0.835 ± 0.003	0.631 ± 0.001
	TGN	0.986 ± 0.001	0.985 ± 0.001	0.911 ± 0.010	0.743 ± 0.030	0.866 ± 0.006	0.843 ± 0.090	0.966 ± 0.001
	CaW	0.976 ± 0.007	$0.988 \pm 2e{-}4$	0.940 ± 0.014	$0.903 \pm 1e{-}4$	0.970 ± 0.001	0.939 ± 0.008	$0.947 \pm 1e{-}4$
	NAT	0.987 ± 0.001	0.991 ± 0.001	0.874 ± 0.004	$0.859 \pm 1e{-}4$	0.924 ± 0.001	0.944 ± 0.002	0.944 ± 0.010
	GraphMixer	0.974 ± 0.001	0.975 ± 0.001	0.835 ± 0.001	0.862 ± 0.003	0.824 ± 0.001	0.932 ± 0.006	$0.935 \pm 3e{-}4$
	Dygformer	0.991 ± 0.0001	0.992 ± 0.0001	0.892 ± 0.005	0.901 ± 0.003	0.926 ± 0.001	0.959 ± 0.001	$0.952 \pm 2e{-}4$
	DyG2Vec	0.995 ± 0.003	$0.996 \pm 2e{-}4$	0.980 ± 0.002	$0.960 \pm 1e{-}4$	0.991 ± 0.001	0.988 ± 0.007	$0.987 \pm 2e{-}4$
	Todyformer	$\mathbf{0.996 \pm 2e{-}4}$	$\mathbf{0.998 \pm 8e{-}5}$	$\mathbf{0.992 \pm 7e{-}4}$	$\mathbf{0.976 \pm 3e{-}4}$	$\mathbf{0.995 \pm 6e{-}4}$	$\mathbf{0.994 \pm 4e{-}4}$	$\mathbf{0.992 \pm 1e{-}4}$
Inductive	JODIE	0.891 ± 0.014	0.865 ± 0.021	0.707 ± 0.029	0.865 ± 0.03	0.747 ± 0.041	0.753 ± 0.011	0.791 ± 0.031
	DyRep	0.890 ± 0.002	0.921 ± 0.003	0.723 ± 0.009	0.869 ± 0.015	0.666 ± 0.059	0.437 ± 0.021	$0.904 \pm 3e{-}4$
	TGAT	0.954 ± 0.001	0.979 ± 0.001	0.805 ± 0.006	0.644 ± 0.002	0.693 ± 0.004	0.820 ± 0.005	0.632 ± 0.005
	TGN	0.974 ± 0.001	0.954 ± 0.002	0.855 ± 0.014	0.789 ± 0.050	0.746 ± 0.013	0.791 ± 0.057	0.904 ± 0.023
	CaW	0.977 ± 0.006	$0.984 \pm 2e{-}4$	0.933 ± 0.014	0.890 ± 0.001	0.962 ± 0.001	0.931 ± 0.002	$0.950 \pm 1e{-}4$
	NAT	0.986 ± 0.001	0.986 ± 0.002	$0.832 \pm 1e{-}4$	0.878 ± 0.003	0.949 ± 0.010	0.926 ± 0.010	0.952 ± 0.006
	GraphMixer	$0.966 \pm 2e{-}4$	$0.952 \pm 2e{-}4$	0.814 ± 0.002	0.821 ± 0.004	0.758 ± 0.004	0.911 ± 0.004	$0.918 \pm 6e{-}4$
	Dygformer	$0.985 \pm 3e{-}4$	$\underline{0.988 \pm 2e{-}4}$	0.869 ± 0.004	$0.942 \pm 9e{-}4$	0.897 ± 0.003	0.945 ± 0.001	$0.931 \pm 4e{-}4$
	DyG2Vec	$\mathbf{0.992 \pm 0.001}$	$\mathbf{0.991 \pm 0.002}$	0.938 ± 0.010	0.979 ± 0.006	0.987 ± 0.004	0.976 ± 0.002	0.978 ± 0.010
	Todyformer	$\underline{0.989 \pm 6e{-}4}$	0.983 ± 0.002	$\mathbf{0.948 \pm 0.009}$	$\mathbf{0.981 \pm 0.005}$	$\mathbf{0.989 \pm 8e{-}4}$	$\mathbf{0.983 \pm 0.002}$	$\mathbf{0.9821 \pm 0.005}$

6.3.2 FLP validation result on TGBL dataset

As discussed in the paper, Todyformer has been compared to baseline methods using the TGBL dataset. Table 9 represents an extension of Table 2 specifically for validation (MRR). The results presented in both tables are in line with counterpart methods outlined in the paper by Huang et al. [2023]. It is important to note that for the larger datasets, TCL, GraphMIxer, and EdgeBank were found to be impractical due to memory constraints, as mentioned in the paper.

Table 9: (Validation) Future Link Prediction performance in Validation MRR on TGB Leaderboard datasets.

| Model	TGBWiki	TGBReview	TGBCoin	TGBComment	TGBFlight	Avg. Rank ↓
Dyrep	0.411 ± 0.015	0.356 ± 0.016	0.512 ± 0.014	0.291 ± 0.028	0.573 ± 0.013	4.2
TGN	0.737 ± 0.004	$\mathbf{0.465 \pm 0.010}$	$\underline{0.607 \pm 0.014}$	0.356 ± 0.019	$\underline{0.731 \pm 0.010}$	2.2
CAWN	$\underline{0.794 \pm 0.014}$	0.201 ± 0.002	OOM	OOM	OOM	3
TCL	0.734 ± 0.007	0.194 ± 0.012	OOM	OOM	OOM	5
GraphMixer	0.707 ± 0.014	0.411 ± 0.025	OOM	OOM	OOM	4
EdgeBank	0.641	0.0894	0.1244	$\underline{0.388}$	0.492	4.6
Todyformer	$\mathbf{0.799 \pm 0.0092}$	$\underline{0.4321 \pm 0.0040}$	$\mathbf{0.6852 \pm 0.0021}$	$\mathbf{0.7402 \pm 0.0037}$	$\mathbf{0.7932 \pm 0.014}$	**1.2**
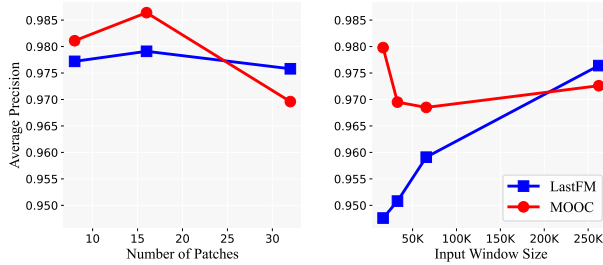
Figure 3: Sensitivity analysis on the number of patches and input window size values on MOOC and LastFM. The plot on the left has a fixed input window size of 262,144, while the one on the right has 32 patches.

Dataset	G. E.	P. E.	Alt. 3	AP
MOOC	✗	✗	✗	0.980
	✓	✗	✗	0.981
	✓	✓	✗	0.987
	✓	✓	✓	**0.992**
LastFM	✗	✗	✗	0.960
	✓	✗	✗	0.961
	✓	✓	✗	0.965
	✓	✓	✓	**0.976**
UCI	✗	✗	✗	0.981
	✓	✗	✗	0.983
	✓	✓	✗	0.987
	✓	✓	✓	**0.993**
SocialEvolution	✗	✗	✗	0.987
	✓	✗	✗	0.987
	✓	✓	✗	0.989
	✓	✓	✓	**0.991**

Table 10: Ablation studies on three major components: global encoder (G. E.), Positional Encoding (P. E.), and number of alternating blocks (Alt. 3)

6.4 Ablation Studies and Sensitivity Analysis

We conducted an evaluation of the model performance across various parameters and datasets to assess the sensitivity of the major hyperparameters. Figure 3 illustrates the sensitivity analysis regarding the window size and the number of patches, with one parameter remaining constant while the other changes. As highlighted in Xu et al. [2020], recent and frequent interactions display enhanced predictability of future interactions. This predictability is particularly advantageous for datasets with extensive long-range dependencies, favoring the utilization of larger window size values to capture recurrent patterns. Conversely, in datasets where recent critical interactions reflect importance, excessive emphasis on irrelevant information becomes prominent when employing larger window sizes. Our model, complemented by uniform neighbor sampling, achieves a balanced equilibrium between these contrasting sides of the spectrum. As an example, the right plot in Figure 3 demonstrates that with a fixed number of patches (i.e., 32), an increase in window size leads to a corresponding increase in the validation AP metric on the LastFM dataset. This trend is particularly notable in LastFM, which exhibits pronounced long-range dependencies, in contrast to datasets like MOOC and UCI with medium- to short-range dependencies.

In contrast, in Figure 3 on the left side, with a window size of 262k, we change the number of patches. Specifically, for the MOOC dataset, performance exhibits an upward trajectory with an increase in the number of patches from 8 to 16; however, it experiences a pronounced decline when the number of patches reaches 32. This observation aligns with the inherent nature of MOOC datasets, characterized by their relatively high density and reduced prevalence of long-range dependencies. Conversely, when considering LastFM data, the model maintains consistently high performance even at 32 patches. In essence, this phenomenon underscores the model's resilience on datasets featuring extensive long-range dependencies, illustrating a trade-off between encoding local and contextual features by tweaking the number of patches.

In table 10, we conduct ablation studies on the major design choices of the encoding network to assess the roles of the three hyperparameters separately: a) Global encoder, b) Alternating mode c) Positional Encoding. Across the four datasets, the alternating approach exhibits significant performance variation compared to others, ensuring the mitigation of over-smoothing and the capturing of long-range

Positional Encoding	Anchor_Node_Mode	Average Precision ↑
SineCosinePos	global target	0.9901
Time2VecPos	global target	0.989
IdentityPos	global target	0.99
LinearPos	global target	0.9886
SineCosinePos	local input	0.9448

Table 11: **Ablation Study on Positional Encoding Options on MOOC Dataset:** This table compares the validation performance at the same epoch across various setups.

dependencies. The outcomes of the single-layer vanilla transformer as global encoder attain the second-best position, affirming the efficacy of our global encoder in enhancing expressiveness. Finally, the global encoder without PE closely resembles the model with only a local encoder (e.i. DyG2Vec MPNN model).

Positional Encoding (PE) Input	Average Precision ↑
without PE	0.9872
random index	0.9873
patch index	0.9889
edge time	0.9886
edge index	0.9877

Table 12: **Ablation Study on the Input of Positional Encoding on MOOC Dataset:** This table compares the validation performance at the same epoch across various types of positions tagged to nodes before PE layer.

6.4.1 Complementary Sensitivity Analysis and Ablation Study

In this section, we have presented the specifics of sensitivity and ablation experiments, which, while of lesser significance in our hyper-tuning mechanism, contribute valuable insights. In all tables, the Average Precision scores reported in the table are extracted from the same epoch on the validation set. Table 13 showcases the influence of varying input window sizes and patch sizes on two datasets. Table 11 illustrates the effects of various PEs, including SineCosine, Time2VecKazemi et al. [2019], Identity, Linear, and a configuration utilizing Local Input as the Anchor Node Mode. The table presents a comparison of results for these different PEs. Notably, the architecture appears to be relatively insensitive to the type of PE used, as the results all fall within a similar range. However, it is worth mentioning that SineCosine PE slightly outperforms the others. Consequently, SineCosine PE will be selected as the primary module for all subsequent experiments. In Table12, an additional ablation study has been conducted to elucidate the influence of positions tagged to each node before

Table 13: Sensitivity analysis on number of patches and target window size

dataset	Input Window size	Number of Patches	Average Precision ↑
LastFM	262144	8	0.9772
LastFM	262144	16	0.9791
LastFM	262144	32	0.9758
MOOC	262144	8	0.9811
MOOC	262144	16	0.9864
MOOC	262144	32	0.9696
LastFM	16384	32	0.9476
LastFM	32768	32	0.9508
LastFM	65536	32	0.9591
LastFM	262144	32	0.9764
MOOC	16384	32	0.9798
MOOC	32768	32	0.9695
MOOC	65536	32	0.9685
MOOC	262144	32	0.9726

being input to the Positional Encoder module. Various mechanisms for adding positions are delineated as follows:

- Without PE: No position is utilized or tagged to the nodes.
- Random Index: An index is randomly generated and added to the embeddings of a given node.
- Patch Index: The index of the patch from which the embedding of the given node originates is used as a position.
- Edge Time: The most recent edge time within its patch is employed as a position.
- Edge Index: The index of the most recent interaction within the corresponding patch is utilized as a position.

As evident from the findings in this table, the validation performance exhibits high sensitivity to the positional encoder's outcomes. Specifically, the model without positional encoder (PE) and the model with random indices manifest the lowest performance among all available options. Consistent with our expectations from previous experiments, the patch index yields the highest performance, providing a compelling rationale for its incorporation into the architecture.

6.5 Computational Complexity

6.5.1 Qualitative Analysis for Time and Memory Complexities

In this section, we delve into the detailed measurement and discussion of the computational complexity of Todyformer. Initially, we adopt the assumption that the time complexity of Transformers is $O(X^2)$ for an input sequence of length X. The primary complexity of Todyformer encompasses both the complexity of the Message Passing Neural Network (MPNN) component and the complexity of the Transformer. To elaborate further, assuming we have a sparse dynamic graph with temporal attributes, we can replace the complexity of MPNNs with $O(l \times (N + E))$, where N and E represent the number of nodes and edges within the temporal input subgraph, and l is the number of MPNN layers for the Graph Neural Network (GNN) tokenizer. In the transformer part, N unique nodes are fed into the Multihead-Attention module. If the maximum length of the sequence fed to the Transformer is N_a, then the complexity of the Multihead-Attention module is $O(N_a^2)$. Notably, N_a is at most equal to M, the number of patches. This scenario occurs when a node appears in all M patches and has interactions in all patches. Consequently, if L is the number of blocks the final complexity is given by:

$$O(L \times l \times (N + E) + L \times N \times M^2) \approx O(N + E) \tag{9}$$

The LHS part of Equation 9 can be simplified to RHS if we assume that L, l, and M^2 are negligible compared to N and E. The RHS of this equation is the time complexity of GNNs for sparse graphs.

6.5.2 Training/Inference Speed

In this section, an analysis of Figure 4 is provided, depicting the performance versus inference time across three sizable datasets. Considering the delicate trade-off between performance and complexity, our models surpass all others in terms of Average Precision (AP) while concurrently positioning in the left segment of the diagrams, denoting the lowest inference time. Notably, as depicted in Figure 4, Todyformer remains lighter and less complex than state-of-the-art (SOTA) models like CAW across all datasets.

6.6 Discussion on Over-Smoothing and Over-Squashing

In Figure 5, the blue curve illustrates the Average Precision performance of dynamic graph Message Passing Neural Networks (MPNNs) across varying numbers of layers. Notably, an observed trend indicates that as the number of layers increases, the performance experiences a decline—a characteristic manifestation of oversmoothing and oversquashing phenomena.

Within the same figure, the red square dots represent the performance of MPNNs augmented with transformers, specifically Todyformer with a single block. It is noteworthy that the increase in
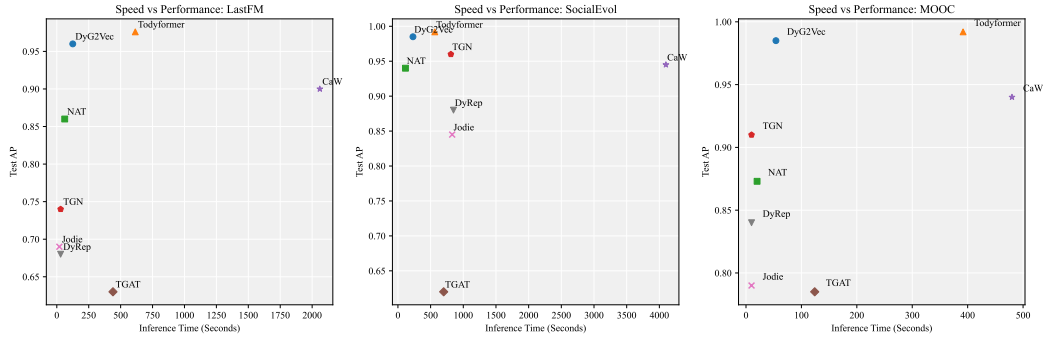
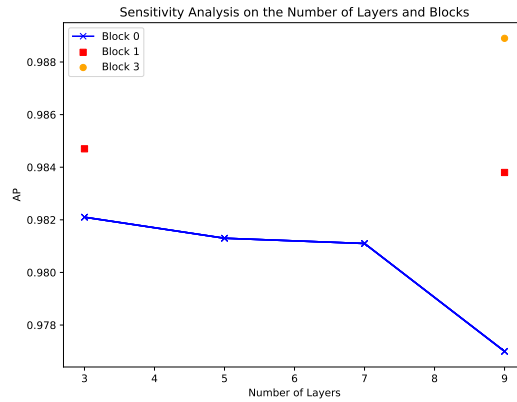Figure 4: The performance versus inference time across LastFM, SocialEvol and MOOC datasets

Figure 5: Sensitivity Analysis on the Number of Layers and Blocks on Mooc Dataset

the number of MPNN layers from 3 to 9 in this configuration results in a comparatively minor performance drop compared to traditional MPNNs.

Furthermore, the yellow circles denote the performance of Todyformer with an alternating mode, where the total number of MPNNs is 9, and three blocks are incorporated. In this setup, a transformer is introduced after every 3 MPNN layers. Strikingly, this configuration outperforms all others, especially those that stack a similar number of MPNN layers without the insertion of a transformer layer in the middle of the architecture. This empirical observation serves as a significant study, highlighting the efficacy of our architecture in addressing oversmoothing and oversquashing challenges.